# Non-uniform flow structure behind a dusty gas shock wave with unsteady drag force

**T. Saito[1], M. Saba[1], M. Sun[2], and K. Takayama[3]**

[1] *Dept. Mechanical Systems Eng., Muroran Institute of Technology, 27-1 Mizumoto-cho, Muroran, 050-8585 Japan*
[2] *Center for Interdisciplinary Research, Tohoku University, 6-3 Aramaki, Aoba-ku, Sendai, 980-8578 Japan*
[3] *Tohoku University Biomedical Engineering Research Organization, Institute of Fluid Science, Tohoku University, 2-1-1 Katahira, Sendai, 980-8577 Japan*

## 1 Introduction

One of the important subjects of high-speed gasdynamics is the two phase flows of gaseous media loaded with small solid particles (dusty gases). The research field is directly linked to many important applications, such as shock wave interactions with solid particles in a solid-fuel-booster nozzle, high speed flight in the rain, snow, or dust, etc. Accordingly, numerous works on the subject have been reported over the last several decades [1–4]. High-speed flows in dusty gases, especially unsteady ones such as those in a dusty gas shock tube, are quite different from their pure gas counterparts due to momentum and energy exchange between gas and solid particles. The solid particles cannot follow rapid changes in the gas velocity and temperature, exhibiting non-equilibrium shock regions behind shock fronts. The objective of this paper is to quantitatively investigate the effect of unsteady drag force on the structure of this non-equilibrium region behind shock waves traveling through a dusty gas.

One of the crucial parts of dusty gas shock tube flows is drag force modeling by which the interaction between gas and solid particles are defined and, in general, even steady drag force formulae for a sphere are used. This practice, however, may cause some errors for extremely time-dependent flows such as highly dust laden strong shock tube flows. Our recent work showed that the drag coefficient of a sphere passing through a shock wave is extremely time-dependent and shows even negative values for certain period of time due to complex wave interactions [5,6]. In this paper, the non-equilibrium region behind the shock wave traveling through a dusty gas is numerically calculated by implementing unsteady drag forces obtained from the work. The significance of the effect of unsteady drag coefficient has been noted and discussed in the past. However, as far as the authors know, not many quantitative investigations on the subject have been reported, and this work is, based on experimental findings, one of very few self-consistent works on the subject.

## 2 Unsteady drag force of a sphere passing through a shock wave

The unsteady drag force acting on a sphere was experimentally measured [5, 6]. In the experiments, an aluminum alloy sphere of 80 mm diameter was suspended by thin wire in a 300 mm x 300 mm vertical shock tube. The test section of the shock tube is filled with atmospheric pressure air at room temperature of 293 K. The shock Mach number Ms is 1.22 and the propagation velocity is 414 m/s. Therefore it takes about 500 $\mu$s for

the shock wave to pass the sphere model. The force acting on the sphere is measured by a piezoelectric accelerometer (Endevco 2250A-10).

Numerical predictions of the drag forces for different sphere diameters, i.e. from 8 $\mu$m to 80 mm, are also carried out. The axisymmetric Navier-Stokes equations with continuity and energy equations are numerically solved. The numerical result for 80 mm diameter is compared with the experimental data for validation and good agreement was obtained.

Figure 1(**a**) is reproduced from [6] and shows unsteady drag forces for different sphere diameters. It is noticed here that the drag coefficient is, in principle, defined for steady flows but in this paper, for the sake of simplicity, we define it as unsteady drag force devided by dynamic force behind the incident shock tube flow. The ordinate of the figure is the drag coefficient of a sphere that is defined as,

$$C_d = \frac{2f}{\rho_0 U_0^2 \pi r^2} \tag{1}$$

where $f$ is the drag force exerted on the sphere and, $r$ the radius of the sphere. The symbols $\rho_0$ and $U_0$, respectively, are the characteristic density and velocity taken as the values behind the incident shock wave in the present case. The abscissa is the time normalized by a characteristic time that is defined by, $r/\sqrt{RT_0}$ or $r\sqrt{\gamma}/a_0$ where $R$ and $\gamma$ are the gas constant and the specific heat ratio, respectively. Symbols $T_0$ and $a_0$ are the temperature and the sound speed ahead of the incident shock wave. The value of $\sqrt{RT_0}$=292 m/s is used throughout the work. The trace with high frequency noises in

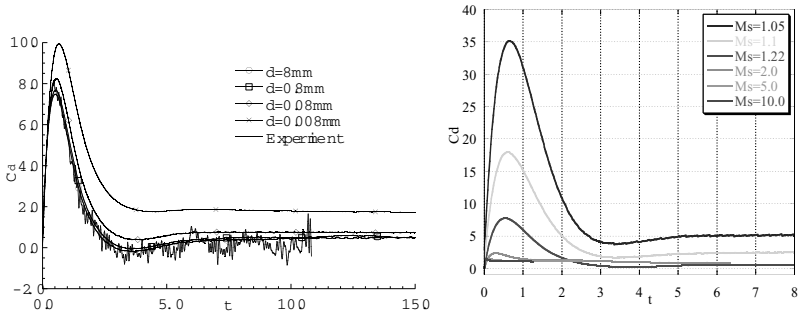


(**a**) (**b**)

**Fig. 1.** Unsteady drag coefficient: (**a**) Experimental and numerical results for different diameters with Ms=1.22, reproduced from [6]; (**b**) Numerical results for different shock Mach numbers with fixed diamter of 8 mm

Fig. 1(**a**) is the experimental data. It is found that the numerical result and the measured data for 80 mm diameter agree quite well and the numerical one is not shown in the figure for clarity. Also the numerical result of 80 mm diameter is nearly the same as 8 mm one. The most pronounced feature of all traces is that the drag coefficient rapidly increases when the shock wave arrives at the front stagnation point of the sphere. It takes a maximum value at around the normalized time t=1, and then falls to a minimum value at t=3 to 4. The value of the minimum is smaller for larger diameter and is even negative for the sphere diameters of 80 mm and 8 mm. The drag coefficient slowly approaches to

its asymptotic value afterwards. In this study, another series of drag force computations for different shock Mach numbers was carried out with a fixed diameter of 8mm. The incident shock Mach numbers are 1.05, 1.1,1.22, 2, 5 and 10 and the results are shown in Fig. 1(**b**).

## 3 Quasi-steady analysis of non-equilibrium region behind the shock wave

### 3.1 Basic equations

Once the velocity and the temperature of gas and solid particles are equilibrated at some distance behind the shock front, the fully developed flow structure of the non-equilibrium region, between the equilibrium region and the shock front, propagates at a constant speed. Then the flow configuration can be regarded as steady relative to the shock front and is numerically obtained by integrating a set of steady equations of mass, momentum and energy conservations [7].

The drag force $D$ and the heat transfer rate $Q$ of a solid particle are expressed via the drag coefficient $C_d$ in Figs. 1 and the Nusselt number Nu as:

$$D = \frac{1}{8}\pi d^2 \rho \left(u - u_d\right) \left|u - u_d\right| C_d \tag{2}$$

$$Q = \frac{\pi d \mu C_p}{\mathrm{Pr}} \left(T - \Theta\right) \mathrm{Nu} \tag{3}$$

where u, T and $C_p$ are the flow velocity, temperature and the specific heat of the gas. The symbols $u_d$, $\Theta$, $C_d$ and $d$ are the velocity, temperature, specific heat and the diameter of solid particles, respectively.

The Nusselt number Nu depend on the particle Reynolds number and determined from the references [8, 9]. The viscosity coefficient is assumed to depend only on temperature and evaluated by Chapman and Cowling [10] and the Prandtl' number Pr is assumed 0.75.

### 3.2 Characteristic scales of dusy-gas flows

Some reference scales characteristic to dusy-gas flows are defined. The characteristic velocity is defined as:

$$u_{\mathrm{ref}} = \frac{a_{f,\mathrm{ref}}}{\sqrt{\gamma}} = \sqrt{\frac{p_{\mathrm{ref}}}{\rho_{\mathrm{ref}}}} = \sqrt{\frac{p_1}{\rho_1}}\,, \tag{4}$$

where the subscript 'ref' indicates the reference state and the values $p_{\mathrm{ref}}$ and $\rho_{\mathrm{ref}}$ are defined from the initial pressure ($p_1 = 101.3$ kPa) and density ($\rho_1 = 1.293$ kg/m$^3$) of the test gas. The symbol $a_{f,\mathrm{ref}}$ referes to the frozen sound speed of the initial state of the test gas. It is shown that the following characteristic quantity $l$ has the dimension of length [2]:

$$l = \frac{8m}{\pi \rho_{\mathrm{ref}} d^2} = \frac{4}{3}\frac{\rho_p}{\rho_{\mathrm{ref}}}\, d = \frac{4}{3}\frac{\rho_p}{\rho_1}\, d, \tag{5}$$

where $\rho_p$ is the particle material density. The reference length $l$ is used as the length scale in this study. Therefore, the reference time is defined as $\tau = l/u_{\mathrm{ref}}$. The ratio of

mass concentrations $\alpha$ and the ratio of the specific heats $\beta$ are difined as characteristic parameters of dusty gases as:

$$\alpha = \frac{\sigma_{\rm ref}}{\rho_{\rm ref}} \ , \quad \beta = \frac{C_m}{C_v} \ , \tag{6}$$

where $\sigma_{\rm ref}$ is the initial mass concentration of the solid particles and $C_v$ is the gas specific heat at constant volume. The value of $\beta$ is assumed to be unity in this study.

## 4 Numerical results and discussions

Structures of nonequilibrium region behind a shock wave front obtained with the steady and the unsteady drag coefficients are calculated. It is observed in Fig. 1 that the drag coefficient varies significantly with time just behind incident shock waves and then approaches to an asymptotic value. We assume that this asymptotic value is the steady drag coefficient and the first series of calculations (Case 1) is obtained with this steady drag coefficient. The second series of calculations (Case 2) is carried out with the unsteady drag coefficients deduced from the experimental and numerical results shown in Fig. 1.

### 4.1 Numerical results for Ms = 1.22

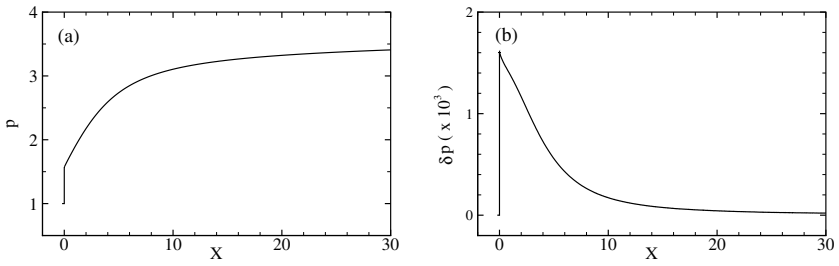


**Fig. 2.** Pressre profiles for Ms=1.22: (**a**) Case 1 and Case 2, (**b**) Difference between Case 1 and Case 2

Figure 2 compares the pressure profiles obtained for Case 1 and Case 2. As expected, the difference between them is so small that the curves of Case 1 and Case 2 overlap with each other in Fig. 2 (**a**). The difference between the two curves is taken and plotted in Fig. 2 (**b**). This way the effect of the unsteady drag coefficients is clearly observed. It takes a maximum value of about 0.16% of the initital pressure behind the incident shock wave.

The gas density and the particle concentration are shown in Fig. 3 in the similar manner as in Fig. 2. It is seen that the difference of the particle concentration between Case 1 and Case 2 takes a maximum not at the shock wave front but at around x=2 while the difference of the gas density takes maximum just behind the shock wave front.

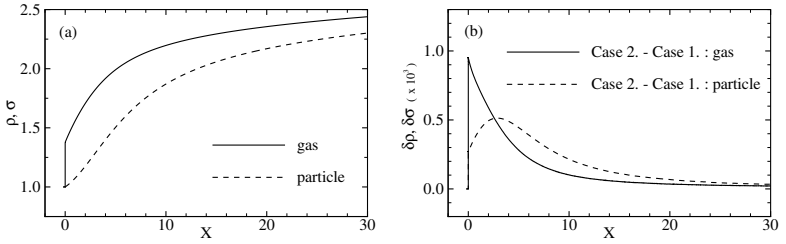


**Fig. 3.** Gas density and particle concentration profiles for Ms=1.22: (**a**) Case 1 and Case 2, (**b**) Difference between Case 1 and Case 2

### 4.2 Numerical results for different Mach numbers

Investigations of the effect of unsteady drag force for different incident shock Mach numbers are carried out. Figure 4 shows the differences of Case 1 and Case 2 in the profiles of gas and particle concentrations. It is seen in Figure 4 (**a**) that $\delta\rho$ has a spike at the front and has a maximum some distance behind the shock front for Ms=1.05. When the shock strength is increased the maximum values occure at shock front. Particle concentration in Case 2 becomes significantly larger than that in Case 1 as the shock Mach number is increased. It is found that the effect of the nominal unsteady drag coefficient is more significant for smaller shock Mach numbers. This is due to the fact that the relative significance of the momentum and energy exchanges between gas and particle phases in the initial stage is less for stronger shock waves.

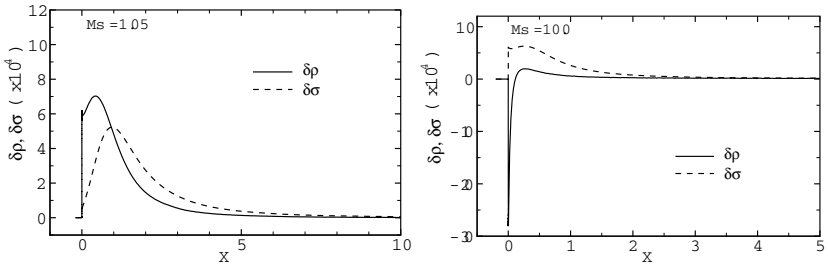


(**a**) (**b**)

**Fig. 4.** Gas and particle concentration for different Mach numbers: (**a**) Ms=1.05, (**b**) Ms=10.; r=4 mm

### 4.3 Numerical results for different mass ratios

The ratio of the particle concentration to the gas density $\alpha$ is an important characteristic parameter. Profiles of flow properties with $\alpha$=10 are calculated and compared with the previous results for $\alpha = 1$. Pressure profiles with $\alpha = 10$ and 1 are compared in Fig. 5. The effect of unsteadiness of the drag coefficient becomes much more significant with increased value of $\alpha$. The pressure difference between Case 1 and Case 2 is more than 4% with $\alpha = 10$ while it is only 0.16 % when $\alpha = 1$.

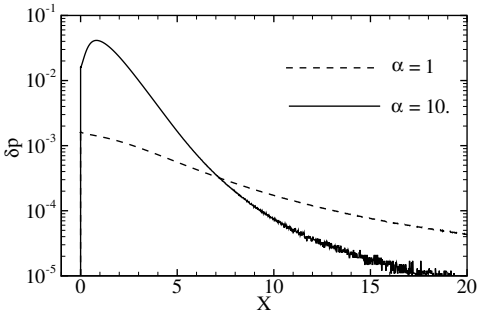


**Fig. 5.** Comparison of pressure profiles with different particle concentrations $\alpha = 1$ and $\alpha = 10$, $r = 4mm$ and Ms=1.22: solid line; $\alpha = 10$, broken line; $\alpha = 1$

## 5 Summary

The effect of time dependency of drag coefficient on dusty gas flows is numerically investigated. Dusty gas flows involve many characteristic parameters and we do not intend to clarify the effect for wide variety of their combinations. Instead, we have quantitatively investigated it for some typical cases including our previous works.

It is found that the effect is more significant for lower shock Mach numbers and higher values of the parameter $\alpha$ that is defined as the ratio of the particle mass concentration to the gas density. In general, when the value of $\alpha$ is of the order of unity, contribution of unsteady drag force to flow structures is less significant. However, for dusty gases with higher loading ratio, the effect of unsteady drag force becomes more significant. We plan to verify the usefulness of the present drag force model by performing series of experiments.

## References

1. Rudinger, G.: Some properties of shock relaxation in gas flows carrying small particles. Phys. Fluids **12**(5), 658–663 (1964)
2. Miura, H., Glass I.I.: On a dusty-gas shock tube. Proc. R. Soc. Lond. A **382**, 373–388 (1982)
3. Igra O., Takayama, K.: Shock tube study of the drag coefficient of a sphere in a nonstationary flow. In: Takayama, K. (ed.) Proc. of the 18th International Symposium on Shock Waves, Sendai, Japan **1**, 491–497 (1991)
4. Saito, T.: Numerical analysis of dusty-gas flows. J. Comput. Phys. **176**, 129–144 (2002)
5. Tanno, H., Itoh, K., Saito, T., Abe, A., Takayama, K.: Interaction of a shock with a sphere suspended in a vertical shock tube. Shock Waves **13**, 191–200 (2003)
6. Sun, M., Saito, T., Takayama, K., Tanno, H.: Unsteady drag on a sphere by shock wave loading. Shock Waves **14**, 3–9 (2005)
7. Saito, T., Marumoto, M., Takayama K.: Numerical investigations of shock waves in gas-particle mixtures. Shock Waves **13**, 299–322 (2003)
8. Gilbert, M., Davis, L., Altman, D.: Velocity lag of particles in linearly accelerated combustion gases. Jet Propulsion **25**, 26–30 (1955)
9. Knudsen, J.G., Katz, D.L.: Fluid mechanics and heat transfer. McGraw-Hill, New York (1958)
10. Chapman, S., Cowling, T.G.: The mathematical theory of non-Uniform gases. Cambridge University Press (1961)